# Rapid inertial solution exchange for enrichment and flow cytometric detection of microvesicles

Jaideep S. Dudani,[1,a)] Daniel R. Gossett,[1,2] Henry T. K. Tse,[1,2,b)] Robert J. Lamm,[1] Rajan P. Kulkarni,[3,4,c)] and Dino Di Carlo[1,2,3,c)]
[1]*Department of Bioengineering, University of California, Los Angeles, Los Angeles, California 90095, USA*
[2]*California NanoSystems Institute, Los Angeles, California 90095, USA*
[3]*Jonsson Comprehensive Cancer Center, Los Angeles, California 90095, USA*
[4]*Division of Dermatology, David Geffen School of Medicine, Los Angeles, California 90095, USA*

(Received 11 December 2014; accepted 29 January 2015; published online 5 February 2015)

Exosomes, nanosized membrane-bound vesicles released by cells, play roles in cell signaling, immunology, virology, and oncology. Their study, however, has been hampered by difficulty in isolation and quantification due to their size and the complexity of biological samples. Conventional approaches to improved isolation require specialized equipment and extensive sample preparation time. Therefore, isolation and detection methods of exosomes will benefit biological and clinical studies. Here, we report a microfluidic platform for inline exosome isolation and fluorescent detection using inertial manipulation of antibody-coated exosome capture beads from biological fluids. © *2015 AIP Publishing LLC*.
[http://dx.doi.org/10.1063/1.4907807]

## INTRODUCTION

Exosomes are small membrane-bound vesicles (30–100 nm) released by cells that have roles in intercellular communication, immunology, viral transfer (including Human Immunodeficiency Virus (HIV)), priming tumors for metastasis, and many other functions.[1–5] They are a subset of cell-derived vesicles including apoptotic bodies and microvesicles. In recent efforts to understand their clinical significance as potential disease biomarkers, exosomes have been found in numerous biofluids including saliva, blood, urine, and bronchoalveolar lavage (BAL) fluid.[6–9] Exosomes are released when multivesicular bodies (MVBs) from the late endosome fuse with the cell membrane. This mechanism results in cellular components (e.g., proteins and RNA) packaged within exosomes and positioning of surface markers on their exterior surfaces.[10–12] Thus, exosomes can carry information about their parent cells of origin, which could provide valuable information about the cells that release them and provide a snapshot of biological activity without accessing parent cells directly. Furthermore, exosomes have been implicated in antigen presentation for various biological functions that can play roles in virology and immunology. In the context of cancer, exosomes are often shed by tumor cells in high numbers. Beyond providing molecular information, exosome concentration has been correlated with increasing tumor mass and grade or severity.[13,14] Accordingly, exosome concentration might be much higher than sparse circulating tumor cells (CTCs), which makes exosomes an attractive alternative as potential prognostic biomarkers.[15]

[a)]Present address: Department of Biological Engineering, Massachusetts Institute of Technology, Cambridge, Massachusetts 02139, USA.
[b)]Present address: CytoVale Inc., South San Francisco, California 94080, USA.
[c)]Authors to whom correspondence should be addressed. Electronic addresses: rkulkarn@ucla.edu, Tel.: (310) 717-1385, Fax: (310) 794-7005 and dicarlo@seas.ucla.edu, Tel.: (310) 983-3235, Fax: (310) 794-5956.

 

Despite the significant interest and widespread implications of exosomes, their clinical utility has been limited and biological roles obscured due to the difficulty in their isolation.[2] The current gold standard for isolation is a label-free method that involves repeated lengthy ultracentrifugation steps, totaling several hours of sample processing. While ultracentrifugation is label-free ensuring no molecular bias in isolation, tetraspanin expression on exosomes has been well-characterized (such as CD63 and CD81).[6] Additionally, epithelial cell adhesion molecule (EpCAM) expression has been found on the surface of some exosomes (specifically tumor-derived exosomes).[14,16] This has enabled novel affinity-based methods exploiting the levels of surface markers on exosomes that can expedite their isolation and potentially provide pure samples. These methods involve either immunomagnetic capture[14] or affinity extraction on the surface of microchannels.[17,18] Immunomagnetic methods require magnetic-activated cell sorting (MACS) separators and also an ultracentrifugation step to account for dilutions that occur during operation.[14] Similarly, the microchannel method also requires an ultracentrifugation step prior to operation for some samples and operates at low flow-rates, limiting the volume of fluid it can process.[17] Both of these techniques additionally do not integrate quantification or detection inline with isolation.

Subsequent to isolation, several methods of quantification and characterization can be employed. These include analysis of protein content, RNA content, surface marker expression, and total count.[6] Accordingly, there is a need to standardize techniques in exosome isolation, handling, detection, and quanitification.[12]

Here, we present a tool for affinity isolation of exosomes that operates at high-throughput (orders of magnitude greater volumes than previously reported microfluidic isolation methods[17,18]) and requires just one benchtop centrifugation step prior to operation, which we utilized to isolate exosomes from various biofluids of interest (e.g., cell culture supernatants and blood). The typical flow rate achieved in our device is greater than five-fold higher than previous methods.[17,18] High-throughput isolation will be crucial for fully dissecting the roles of exosomes in various biological contexts. Finally, we integrated an inline fluorescence detection system for immediate detection of exosomes.

## MATERIALS AND METHODS

### Device fabrication

Fabrication was carried out using standard photolithography and replica molding techniques.[19] The computer-aided design drawing depicted in supplementary Figure 1(A)[29] was used to make a mask for exposure to photoresist spun on to silicon wafers. This master mold was cast with (poly)dimethylsiloxane (PDMS) (Sylgard 184 Silicone Elastomer Kit; Dow Corning Corp., Midland, MI, USA). PDMS was cured for several hours then cut, punched at inlet and outlet ports, air plasma treated, and bonded to glass. Devices were placed in the oven for at least one hour before use.

### Device operation

For all experiments involving the device, fluid was introduced using PHD 2000 syringe pumps (Harvard Apparatus, Holliston, MA, USA) through Polyetheretherketone (PEEK) tubing. For experiments not involving flow cytometry, the device was monitored under a microscope-connected to a high-speed camera (Phantom v711, Vision Research, Inc., Wayne, NJ, USA). For more in depth understanding of device operation and operating principles, refer to the initial description and characterization of RInSE.[20]

### Exosome capture beads

20 $\mu$m polystyrene beads with streptavidin conjugated surfaces (Micromod, Rostock, Germany) were incubated with biotinylated anti-human CD63 (Biolegend, Inc., San Diego, CA, USA) for 30 min at 37 °C. After incubation, the beads were centrifuged and resuspended in tris-buffered saline (TBS) until they were used.

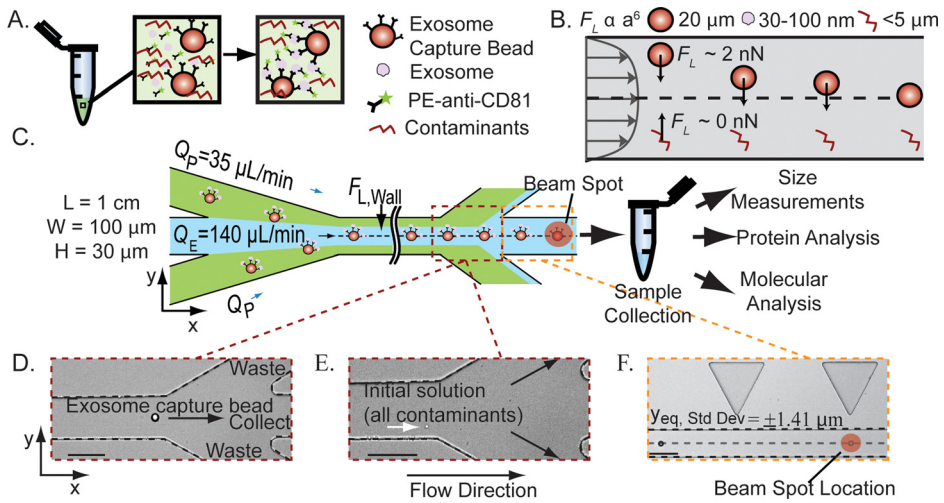


FIG. 1. Exosome isolation and detection using rapid inertial solution exchange. (a) The biofluid of interest is incubated with exosome capture beads. For inline detection, PE-anti-CD81 is also added. (b) Cross section of RInSE showing equilibrium positions of beads in the middle of the microchannel. (c) After incubation, beads are injected into the microfluidic system with a coflow of TBS. Inertial lift forces cause the particles to migrate across fluid streamlines into the exchange buffer. (d) High speed image of exosome capture bead being collected. (e) High speed image showing that contaminants are siphoned off. White arrow indicates a non-exosomal microvesicle. (f) High speed image of inline detection region of RInSE. Scale bar = 100 $\mu$m.

### Cell culture and blood collection

Cells were maintained in culture in Roswell Park Memorial Institute (RPMI) media (melanoma cells) or Dulbecco's Modified Eagles Media (DMEM) for breast cancer cells supplemented with 10% fetal bovine serum (FBS) (Thermo Fisher Scientific, Inc., Waltham, MA, USA) and 1% Penicillin- Streptomycin (Invitrogen Corp., Carlsbad, CA, USA). Cells were passaged once they reached 70% confluence. For all isolation experiments, the media was replaced with media containing exosome-depleted FBS (Exo-FBS, Systems Biosciences, Mountain View, CA) the day before exosome isolation to ensure that isolated exosomes originated from the cell line. Culture supernatant was collected and centrifuged at 10 000 rpm for 10 min to eliminate dead cell debris prior to adding exosome capture beads. Blood was drawn from consenting donors according to a protocol approved by the UCLA Institutional Review Board.

### Bead incubation

Beads suspended in a small volume of TBS were added to the culture supernatant and kept at 4 °C to minimize non-specific binding. The sample was mixed periodically to ensure homogeneity. For experiments involving flow cytometry, phycoerythrin (PE)-anti-human CD81 (Biolegend, Inc., San Diego, CA, USA) was added 30 min prior to device operation to avoid antibody cross-reactivity and have two molecular markers of exosomes.

### Characterizing rapid inertial solution exchange (RInSE) purity and efficiency

To determine solution exchange purity and efficiency, 19 $\mu$m polystyrene beads suspended in trypan blue (Thermo Fisher Scientific, Inc., Waltham, MA, USA) were pumped into RInSE at 70 $\mu$l/min while TBS was pumped in as the exchange solution at 140 $\mu$l/min. At these flow rates, the particle Reynolds Number, $Re_p = \rho U a^2/\mu D_h$, equals 10, where $\rho$ is fluid density, $U$ is fluid velocity, $a$ is particle diameter, $\mu$ is dynamic viscosity of the fluid, and $D_h$ is hydraulic diameter of the channel. The channel Reynolds Number, $Re_c = \rho U D_h/\mu$, is 54. The beads were transferred into the exchange solution and transfer efficiency was measured by monitoring bead collection into the collect channel. Efficiency is defined by the number of beads collected divided by total beads observed at the collect/reject junction. Exchange solution purity was also

measured using a spectrophotometer measuring absorbance at $\lambda = 607$ nm. The absorbance of the exchange solution collected was 0 using TBS as a blank. A standard curve with trypan blue was made ranging from 100% to 1% trypan blue. The spectrophotometer was sensitive in the whole range of trypan blue suggesting that if there was any solution contamination in the collection channel, then there would be less than 1% of contamination.

### Staining of rejected microvesicles

After RInSE operation, solution was collected and centrifuged down to determine if larger microvesicles were also collected. Nile red was added to the solution collected. Nile red fluoresces (excitation: 485 nm, emission: 525 nm) when it binds to lipids in membranes.

### Flow cytometry experiments

A simplified flow cytometer set up was built to interface with RInSE as seen in supplementary Figure 3.[29] A 532 nm laser was focused onto the microfluidic channel through an objective (10× DIC, Nikon Instruments, Inc., Melville, NY, USA). Light was collected back through the objective and filtered with a band-pass filter with a center wavelength of 575 nm and full width half maximum of 40 nm (Chroma Technology Corp., Bellows Falls, VT, USA). Filtered light was collected into a photomultiplier tube (PMT) (H10723-01; Hamamatsu City, Shizuoka, Japan). The signal was digitized by a digitizer (National Instruments, Austin, TX, USA) at a sampling rate of 1 MS/s. Lowpass filtering was performed on the digitized signal in MATLAB (The MathWorks, Inc., Natick, MA, USA) to remove high-frequency noise on the fluorescence signal. The initial suspension containing cell culture supernatant, exosome capture beads, and PE-anti-human CD81 was pumped into the device with a coflow of TBS. The beam spot was positioned in the collection channel, which allowed enough time for capture beads to migrate and order into the exchange solution.

### Size measurements

Collected beads were centrifuged at 2500 rpm for 5 min. The supernatant was collected and analyzed in parallel to assess if anything was nonspecifically collected. Beads were resuspended in IgG elution buffer for 10 min. After 10 min, beads were centrifuged at 2500 rpm for 5 min. The eluted exosomes were measured using a Malvern Zetasizer Nano ZS model Zen 3600 (Malvern Instruments, Inc., Westborough, MA) with a dispersant refractive index of 1.33 to reflect water and a sample refractive index of 1.44 as suggested by the manufacturer. For analysis, the Malvern General Purpose Analysis was used.

## RESULTS AND DISCUSSION

Our technique employs a microfluidic system that utilizes inertial lift forces at finite Reynolds number to position microparticles and exchange the solution around them. This technique, termed RInSE,[20] is used to isolate and detect exosomes inline by transferring affinity microbeads incubated with a biofluid of interest into a wash buffer (Figure 1). Solution exchange on-chip is able to eliminate several spin-wash steps typically required and enable high signal-to-noise flow cytometric detection. Importantly, device manufacturing is simple and microparticle manipulation is passive (requiring no external forces for microparticle transfer). For the work presented here, a computer-aided design of the channels was used to make a master mold using photolithography techniques (supplementary Figure 1(A)).[29] Devices were cast in PDMS.

Exosome samples (melanoma cell culture or breast cancer cell culture supernatant) were centrifuged at 10 000 rpm for 10 min to remove dead cells and then the supernatant incubated with affinity-capture polystyrene beads (diameter = 20 $\mu$m) for several hours at 4 °C before injecting into RInSE at Q = 70 $\mu$l/min via a syringe pump (Figure 1(a)). At finite Reynolds number in a high aspect ratio microchannel (width (W) $\gg$ height (H)), particles experience a lift force ($F_L \propto a^6/H^4$, a = diameter), which forces particles to the channel centerline. Typical

acellular contaminants are $<5\,\mu$m in size and thus experience negligible lift force whereas the exosome capture beads ($20\,\mu$m) experience a lift force of approximately 2 nN and migrate at rates of approximately $5\,\mu$m/s (Figure 1(b)). Simultaneously, an exchange solution of TBS was pumped into another inlet at a higher volumetric flow rate such that it occupied the majority of the channel ($Q = 140\,\mu$l/min). The beads entered the main transfer channel where the co-flow was established. The transfer channel of RInSE is a high-aspect ratio rectangular channel (width $= 100\,\mu$m, height $= 30\,\mu$m). In these high-aspect ratio channels, the particle equilibrium positions lie in the middle of the wide face of the channel due to a diminished shear gradient in the center of the channel.[20] The beads passively migrate into the exchange solution due to the inertial lift forces. After solution exchange, inline detection with a custom-built fluorescence detection scheme is possible and exosome capture beads can be collected and exosomes eluted or lysed for downstream analysis (Figures 1(c) and 1(d)). The initial exosome-containing solution and all contaminants were siphoned off to waste channels (Figure 1(e)). Blood samples were processed similarly after red blood cell lysis.

Importantly, inertial focusing aligns microbeads for flow cytometry when flowing at similar rates used for transfer, which enables RInSE to be an integrated tool.[20–22] For fluorescence measurements, PE anti-CD81 (excitation: 546 nm, emission: 578 nm) was added to the bead/exosome suspension for 30 min after the 4-h incubation. Bead positioning was very precise, having a standard deviation of only $1.41\,\mu$m in the y direction ($n = 10$, $20\,\mu$m diameter polystyrene beads), which is well within tolerance of commercial flow cytometers (Figure 1(f)).[23]

We characterized the device to ensure the exchange solution remained pure and exosome capture beads were not moving into the waste channels. Trypan blue was injected into the first inlet and TBS was injected as the exchange solution. Absorbance measurements revealed no trypan blue was present in the output of the collection channel. This is possible by having limited diffusion within the system to prevent solution contamination in this high Peclet number system ($>10^5$). Additionally, bead collection efficiency into the collection channel (beads in collect channel/beads observed $\times$ 100) was 100% (supplementary Figure 1(B)).[29] We also found that large microvesicles (non-exosomal membrane bound vesicles) were not large enough to transfer ($\sim 1\,\mu$m) into the collect stream. Additionally, exosome-capture beads did not isolate these larger vesicles as determined by microscopic observation of beads and staining of large microvesicles. Staining of the solution from the waste channels showed presence of large membrane bound vesicles ($1\,\mu$m) that were not collected with the beads. These results highlight the potential advantage of this technique as it can result in a highly pure sample of beads in a clean buffer.

We utilized this method to enrich exosomes using anti-CD63 capture beads (for melanoma culture supernatant) and anti-EpCAM capture beads (for breast cancer culture supernatant and healthy donor blood). We first characterized the system for isolation and detection of exosomes from the supernatant of melanoma cell line cultures. We also demonstrated the ability to isolate exosomes from more complex biological fluids, by isolating and detecting exosomes from MCF7 cells and blood using the inline detection system (supplementary Figures 2(A) and 2(B)).[29] The system is modular to enable the use of a range of antibodies for specific exosome capture and detection.

We next characterized the isolated exosomes to ensure we were enriching for exosomes selectively. Exosomes from melanoma cells were isolated into a solution of TBS. After collection, IgG elution buffer was added to release exosomes off the beads (Figure 2(a)).[14] Size characterization using dynamic light scattering (DLS) on a Malvern Zetasizer showed that collected samples were within the expected size range of exosomes ($75.4 + 15.5$ nm). The inlet suspension had a maximum peak at $3.1 + 0.8$ nm demonstrating that our system enriched selectively from this background solution (Figure 2(b)). Repeating the isolation with control streptavidin coated polystyrene beads showed that resulting sample did not contain particles in the size range of exosomes. The peak for streptavidin control isolation was 0.31 nm, which is outside of the true detection range of the instrument and therefore the streptavidin alone does not contribute to the true exosome sizes detected. This suggests that RInSE selectively collects exosomes from a background solution.

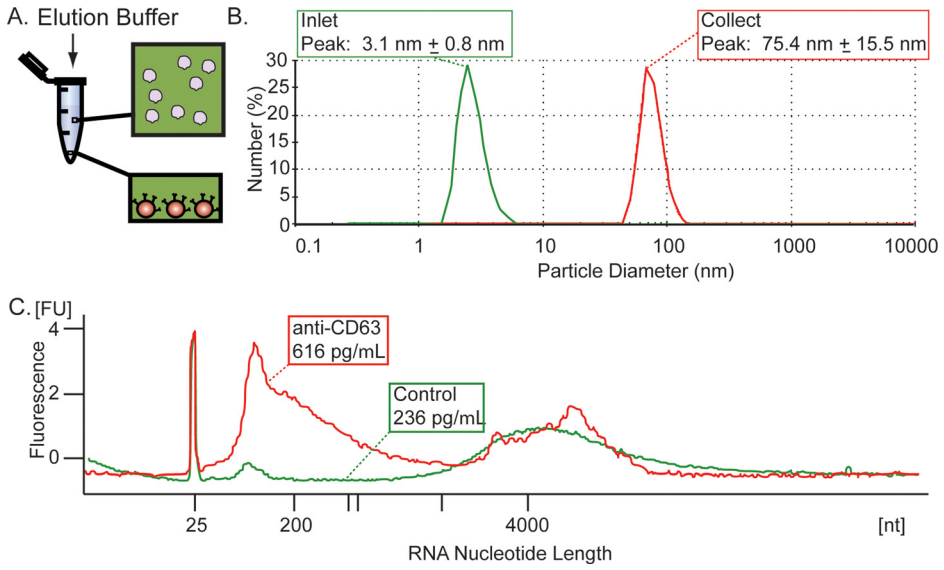


FIG. 2. Characterization of isolation. (a) Schematic of elution for size measurements. (b) DLS measurements from melanoma exosomes collected with anti-CD63 beads and the inlet size measurements. Inlet solution peak is due to background low concentration and polydispersity. Collect solution of melanoma exosomes isolated with anti-CD63 beads show corresponding enrichment for exosome-sized vesicles. C. RNA measurements from control bead isolation show a much lower RNA content extraction than with the anti-CD63 capture beads. RNA measurements from anti-CD63 bead isolation show a range of sizes collected that correlate with miRNAs and mRNAs. There seems to be some content at large sizes that might be due to non-specific adsorption of free floating RNA from lysed cell material present in the serum or growth media. Overall RNA quantity is also increased with anti-CD63 isolation. 25 nt peak is internal control.

We additionally characterized the RNA content from the isolated exosomes to demonstrate that RInSE selects for exosomes. RNA was extracted from isolated exosomes using an RNAqueous Micro Kit. RNA content was measured by a 2100 Bioanalyzer Eukaryote Total RNA Pico chip. The standard RNA purification protocol was modified to better isolate small RNA fragments as recommended by the manufacturer's instructions. For these experiments, melanoma cell supernatants from the same number of cells were incubated with anti-CD63 capture beads and control beads. RNA was extracted from both samples into a 20 $\mu$l volume.

RNA extracted with the anti-CD63 beads were of a range of sizes including small size RNA, representing microRNAs (miRNA) and messengerRNAs (mRNA), which have been shown to be a large composition in exosomes (Figure 2(c)).[2] Control bead isolation resulted in much lower RNA extracted (2.6 fold) than with anti-CD63 beads (Figure 2(c)). Between the anti-CD63 beads and the control beads, there was an increase in the smaller RNA size fragments (<200 nucleotides (nt), peak height 9 fold greater) of the size of mRNAs and miRNAs likely present in exosomes demonstrating that this method selectively isolated exosomes. The peak at 25 nt is an internal Bioanalyzer standard. There was some nonspecific adsorption in both the control and anti-CD63 beads at large nt values. This might be associated with large RNA fragments from lysed cells (e.g., ribosomal RNA). This can be mitigated by more thorough, nonfouling coatings on the beads to minimize nonspecific adsorption of free-floating RNA. Isolation of exosomes and subsequent characterization of RNA contained within exosomes using this method would enable enhanced understanding of the functional role of exosomes.

Using the melanoma culture supernatant, we confirmed that concentration dependent isolation of exosomes was feasible. We demonstrated this by performing inline measurements using a custom simplified flow cytometer (supplementary Figure 3),[29] which can also enable our tool to quantify exosomes. Briefly, a 532 nm laser was focused through an objective onto the microchannel, fluorescence measurements are band-pass filtered, focused, and collected on a PMT. Since there are two focal positions in RInSE for bead positioning, the beam spot was aligned in the middle of the two positions. To accomplish this, envy green-labeled polystyrene beads (excitation: 525 nm, emission: 565 nm) were introduced into RInSE and the laser was aligned until

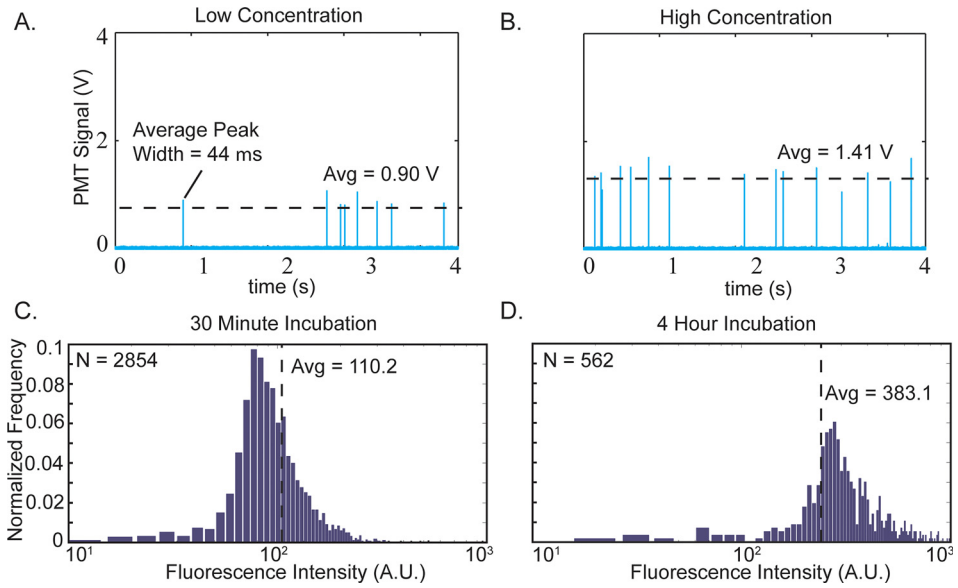


FIG. 3. Cytometric detection of exosomes. (a) and (b) Average signal from a high exosome concentration solution was correlated with higher average peak intensity as compared to the lower concentration solution using the RInSE Cytometer. Each peak is an individual bead passing through the beam spot. (c) and (d) Histogram plots of fluorescent intensity of exosome capture beads isolated by RInSE and analyzed using a commercial flow cytometer for melanoma cell exosome isolation and detection. Longer incubation time of beads resulted in higher average intensity. Incubation time with anti-CD81 was identical for both samples.

a uniform signal was obtained before introducing exosome-capture beads. The beam spot was aligned such that the signal from the envy green beads was constant. The signal was digitized and analyzed using a custom written MATLAB code for signal analysis, peak finding, and peak analysis.

To demonstrate the ability of our system to distinguish differences in exosome concentration, the same number of beads and concentration of PE-anti-CD81 were incubated with samples containing different concentrations of supernatants (two orders of magnitude difference) from melanoma cells in culture by diluting various supernatant concentrations in the same volume of PBS. The average signal peak for beads associated with higher concentration was $1.41 + 0.19\,\text{V}$, compared to $0.90 + 0.10\,\text{V}$ for the lower concentration (Figures 3(a) and 3(b)). This difference was statistically significant (Student t-test, $p < 0.05$). The average beads transit time through the beam spot was $44\,\mu\text{s}$, which is as expected for a $20\,\mu\text{m}$ bead travelling across a $\sim 50\,\mu\text{m}$ beam spot at $\sim 1\,\text{m/s}$. Currently, the system cannot detect small differences, which could be addressed by utilizing a higher power laser and enhancing focusing of the beads. The current system results in two equilibrium positions at the center of the wide face of the channel, which might contribute to the decreased sensitivity. Integration of RInSE with a single-particle focusing system might increase sensitivity and enable the system to detect smaller differences in exosome concentration to monitor disease progression.[23–25] Additionally, recent efforts have demonstrated that elasto-inertial focusing has the possibility to achieve single-particle focusing with exceptional throughput, which might be amenable to integration with RInSE based detection.[26–28] To further validate the RInSE Cytometer we compared our results with those of a commercial flow cytometer. We additionally wanted to test if shorter bead incubation time in the biofluid of interest would be feasible. Cell culture supernatants were incubated with the capture beads for either 30 min or 4 h and then incubated with PE-anti-CD81 for 30 additional minutes. The beads were isolated using RInSE and then analyzed using a BD FACSCalibur. Data were gated to include beads and then fluorescent intensity was measured. Thirty minute incubation of beads resulted in a lower average signal (Figure 3(c)) as compared to a 4 h incubation (Figure 3(d)). This validates that the RInSE cytometer is detecting exosomes but also shows that longer incubation time is necessary for improved antibody binding and capture. In

practice, the system can be operated in batches with incubation of all samples at the same time and quick operation of the device for multiple samples. RInSE's ability to isolate and report on the concentration of exosomes in a single step might enable the exploration of exosomes for clinical biomarker for disease. Additionally, the ability for facile isolation will prove to be important for enhanced study in the field.

## CONCLUSIONS

We have developed a novel, rapid tool that uses inertial manipulation of antibody coated beads for rapid exosome isolation from biofluids. Actual operation time is just several minutes following a short centrifugation step compared to 5–7 centrifugation steps in conventional procedures, thereby minimizing dedicated equipment time needed. Additionally, this method has been directly coupled to inline laser detection of fluorescently labeled exosomes. We have demonstrated that this technique yields an enriched population of exosomes, thereby enabling further investigation in this field. We envision this technology will be adopted for facile exosome isolation for research and for quantification as a prognostic or diagnostic tool.

Exosomes are of increasing interest to individuals studying cancer progression, HIV, immunology, and cell signaling but their study has been hindered by a lack of enabling technologies for their isolation and analysis. The ability of the system presented here to be coupled upstream or downstream of other systems makes it particularly attractive for on-chip studies of exosomes after isolation. Also, a single system for isolation and quantification that is feasible with RInSE would allow a higher volume of clinical samples to be processed to determine the utility or feasibility of exosomes as a prognostic biomarker to complement work being done with other systemic prognostic or diagnostic biomarkers.

## ACKNOWLEDGMENTS

The authors would like to thank James Che (UCLA) for assistance with RNA isolation, the UCLA Clinical Microarray Core, the UCLA Flow Cytomery Laboratory, and Jerry Wu (UCLA) for assistance with fluidic modeling and helpful discussion. This work was partially supported by a Goldwater Scholarship (J.S.D.) and a grant from the Howard Hughes Medical Institute to UCLA through the Precollege and Undergraduate Science Education Program (J.S.D.).

[1]F. F. van Doormaal, A. Kleinjan, M. Di Nisio, H. R. Büller, and R. Nieuwland, Neth. J. Med. **67**, 266 (2009); available at http://www.ncbi.nlm.nih.gov/pubmed/19687520.
[2]A. V. Vlassov, S. Magdaleno, R. Setterquist, and R. Conrad, Biochim. Biophys. Acta, Gen. Subj. **1820**, 940–948 (2012).
[3]S. Mathivanan, H. Ji, and R. J. Simpson, J. Proteomics **73**, 1907 (2010).
[4]M. Mittelbrunn and F. Sánchez-Madrid, Nat. Rev. Mol. Cell Biol. **13**, 328 (2012).
[5]H. Peinado, M. Alečković, S. Lavotshkin, I. Matei, B. Costa-Silva, G. Moreno-Bueno, M. Hergueta-Redondo, C. Williams, G. García-Santos, C. M. Ghajar, A. Nitadori-Hoshino, C. Hoffman, K. Badal, B. A. Garcia, M. K. Callahan, J. Yuan, V. R. Martins, J. Skog, R. N. Kaplan, M. S. Brady, J. D. Wolchok, P. B. Chapman, Y. Kang, J. Bromberg, and D. Lyden, Nat. Med. **18**, 883 (2012).
[6]C. Théry, S. Amigorena, G. Raposo, and A. Clayton, Curr. Protoc. Cell Biol. **30**, 3.22.1–3.22.29 (2006).
[7]C. S. Lau and D. T. W. Wong, PLoS One **7**, e33037 (2012).
[8]V. Palanisamy, S. Sharma, A. Deshpande, H. Zhou, J. Gimzewski, and D. T. Wong, PLoS One **5**, e8577 (2010).
[9]M.-P. Caby, D. Lankar, C. Vincendeau-Scherrer, G. Raposo, and C. Bonnerot, Int. Immunol. **17**, 879 (2005).
[10]S. Keller, M. P. Sanderson, A. Stoeck, and P. Altevogt, Immunol. Lett. **107**, 102 (2006).
[11]C. Thery, L. Zitvogel, and S. Amigorena, Nat. Rev. Immunol. **2**, 569 (2002).
[12]C. Beyer and D. S. Pisetsky, Nat. Rev. Rheumatol. **6**, 21 (2010).
[13]M. Logozzi, A. De Milito, L. Lugini, M. Borghi, L. Calabrò, M. Spada, M. Perdicchio, M. L. Marino, C. Federici, E. Iessi, D. Brambilla, G. Venturi, F. Lozupone, M. Santinami, V. Huber, M. Maio, L. Rivoltini, and S. Fais, PLoS One **4**, e5219 (2009).
[14]D. D. Taylor, C. Gercel-Taylor *et al.*, Gynecol. Oncol. **110**, 13 (2008).
[15]B. Mostert, S. Sleijfer, J. A. Foekens, and J. W. Gratama, Cancer Treat. Rev. **35**, 463 (2009).
[16]B. J. Tauro, D. W. Greening, R. A. Mathias, S. Mathivanan, H. Ji, and R. J. Simpson, Mol. Cell. Proteomics **12**, 587–598 (2012).
[17]C. Chen, J. Skog, C.-H. Hsu, R. T. Lessard, L. Balaj, T. Wurdinger, B. S. Carter, X. O. Breakefield, M. Toner, and D. Irimia, Lab Chip **10**, 505 (2010).
[18]Z. Wang, H. Wu, D. Fine, J. Schmulen, Y. Hu, B. Godin, J. X. J. Zhang, and X. Liu, Lab Chip **13**, 2879 (2013).
[19]D. Duffy, J. C. McDonald, S. Olivier, and G. Whitesides, Anal. Chem. **70**, 4974 (1998).
[20]D. R. Gossett, H. T. K. Tse, J. S. Dudani, K. Goda, T. A. Woods, S. W. Graves, and D. Di Carlo, Small **8**, 2757–2764 (2012).

[21]S. C. Hur, H. T. K. Tse, and D. Di Carlo, Lab Chip **10**, 274 (2010).
[22]D. Di Carlo, Lab Chip **9**, 3038 (2009).
[23]H. Shapiro, *Practical Flow Cytometry*, 4th ed. (Wiley-Liss, New York, 2003).
[24]A. Chung, D. Gossett, and D. Di Carlo, Small **9**, 685 (2013).
[25]A. Chung, D. Pulido, J. C. Oka, H. Amini, M. Masaeli, and D. Di Carlo, Lab Chip **13**, 2942–2949 (2013).
[26]E. J. Lim, T. J. Ober, J. F. Edd, S. P. Desai, D. Neal, K. W. Bong, P. S. Doyle, G. H. McKinley, and M. Toner, Nat. Commun. **5**, 4120 (2014).
[27]E. J. Lim, T. J. Ober, J. F. Edd, G. H. McKinley, and M. Toner, Lab Chip **12**, 2199 (2012).
[28]S. Yang, J. Y. Kim, S. J. Lee, S. S. Lee, and J. M. Kim, Lab Chip **11**, 266 (2011).
[29]See supplementary material at http://dx.doi.org/10.1063/1.4907807 for figures describing microchannel design, flow cytometry setup, and detection of exosomes in blood samples and conditioned breast cancer media.